# Validation of Efficiency Maps of an Outer Rotor Surface Mounted Permanent Magnet Machine for Evaluation of Recyclability of Magnets

Adolfo Garcia Gonzalez[1], Amit Kumar Jha[2], Ziwei Li[3], Pranshu Upadhayay[3], and Peter Rasmussen[1]
[1]Department of Energy Technology, Aalborg University, Aalborg 9220 Denmark
[2]G2Elab Grenoble INP, Grenoble 38031 France
[3]VALEO Electrical Systems, Creteil 94000 France

**The goal of this paper is proposing a methodology for the evaluation of the recyclability criterion of permanent magnets (PMs) in electrical machines for Hybrid and Electric Vehicles ((H)EVs). Such methodology was validated with measurements performed to a PM machine of the hub type. In addition, the methodology proposed here is approached in terms of energy consumption. Hence, measurements of torque and speed were taken at various working points. This study comprises the disassembly of one unit in order to determine the main dimensions of the machine for modelling in 2D Finite Element Method (FEM). Additionally, samples of the magnets in the rotor were taken for characterization of their properties. The results of simulations were contrasted with the measurements for the validation of the efficiency maps. Finally, a study case was selected, in which the use of recycled magnet material was simulated and the reduction of efficiency was quantified.**

*Index Terms*—**Efficiency maps, 2D-FEM, driving cycle, energy consumption, magnet recyclability.**

## I. Introduction

THE global trend towards the implementation of (H)EVs is challenging from the perspective of energy supply and the use of materials with high fluctuation of prices in the international market such as Rare Earth Elements (REEs). Recycling of REEs has been proposed as an alternative for counteracting this situation. Furthermore, work has been carried out in the design of electrical machines with recycled materials [1], [2], [3]. However, there is a lack of tools allowing to determine the feasibility of the recycling of PMs in electrical machines. Hence, this article attempts to set the base for a methodology for evaluating of the recyclability of their PMs [4]. In this regard, two approaches might be adopted. One from the perspective of the disassembling process [5], [6]. The second one from the perspective of the energy consumption in the life cycle of the machine. The evaluation of the energy consumption of a machine used in (H)EVs may be done under any of the defined driving cycles [7]. Therefore, it is required to determine the efficiency of the machine at any given working point. In this sense, the methodology proposed here is validated with measurements performed to an outer rotor surface mounted PM machine of the hub type commercially available and used in both electrical scooters and small city cars.

Efficiency maps have shown to be useful at representing the performance of electrical machines in propulsion applications [8]. In addition, work has been carried out with efficiency maps as optimization tool [9]. Furthermore, the analysis of different machines under various driving cycles have been addressed in earlier studies [10]. However, the work presented here is aimed to validate a methodology for the evaluation of the recyclability criterion from an economic perspective (i.e. energy consumption).

Experimental results focused on the determination of efficiency of the machine are presented in Section II. In section III results of simulations are included, as well as, the elaboration of the efficiency maps. Section IV is devoted to the determination of the efficiency maps in a study case assuming the use of recycled magnets. The analysis of the results obtained are shown in section V. Lastly, conclusions are drawn and future work is proposed.

## II. Experimental set-up

Measurements were performed on an outer rotor surface mounted PM which is generally used in electrical scooters or small city cars [11]. The set-up is shown in figure 1. A resistive load was connected to the machine operating as generator, and values of input and output power were measured. The results of efficiency at different values of torque and speed are illustrated in figure 2.


Fig. 1: Experimental set-up.

### A. Disassembly

The disassembly of the machine was carried out in order to obtain the main dimensions for the elaboration of the 2D

Corresponding author: A Garcia Gonzalez. (email: agg@et.aau.dk). "A. Garcia Gonzalez, A. Kumar Jha, Z. Li, P. Upadhayay and P. Rasmussen contributed equally."

FEM model. Samples of the magnets were taken and analysed with the Physical Property Measurement System (PPMS) from Quantum Design®.

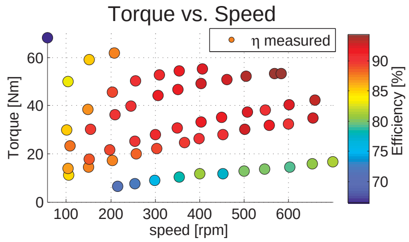


Fig. 2: Measured efficiency at different values of torque and speed.

(a)

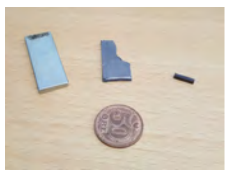

(b)

Fig. 3: (a) Disassembly process, (b) Magnet samples.

### B. Main dimensions

The main dimensions of the outer rotor machine analysed in this study are shown in table I.

TABLE I: Main machine dimensions.

| Parameters | Value |
|---|---|
| Stack length $L_{stack}$ [mm] | 40 |
| Maximum speed [rpm] | 700 |
| Air-gap length [mm] | 0.6 |
| Magnet axial length [mm] | 40 |
| Magnet thickness [mm] | 3 |
| Magnet width [mm] | 14 |
| Stator radius [mm] | 126.5 |
| Number of poles | 56 |
| Number of slots | 63 |
| Winding type: concentrated | |

## III. Elaboration of efficiency maps

Figure 4 illustrates the model implemented in 2D FEM. In addition to the dimensions in table I, the properties of the materials were required as inputs. The test performed to the magnet with PPMS yielded a value of remanence of approximately $B_r = 1.2$ T. On the other hand, the quality of the material of the stator laminations was unknown. Nevertheless, the properties of a standard SiFe lamination with similar thickness were modelled. Hence, the lamination M400-50 was selected. Simulations were run applying the measured current. The efficiency of the measured working points was estimated with the calculated no-load losses (i.e. stator and rotor iron losses and PM losses) and copper losses. The effect of harmonics induced by the modulation of the inverter were disregarded in the simulations. The results are shown in figure 5. Most of the results follow the trend of the measurements illustrated in figure 2.

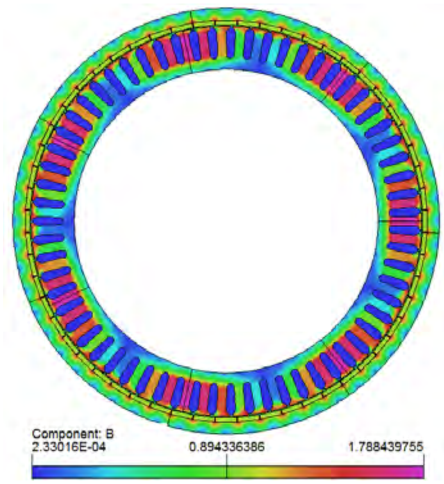


Fig. 4: Geometry modelled in FEM and magnetic flux density distribution at T=11.6 Nm and n=105 rpm.

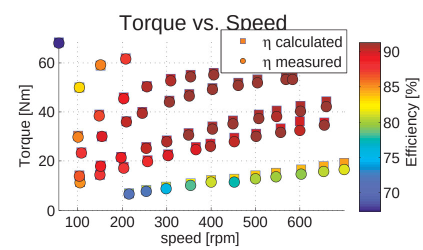


Fig. 5: Measured and calculated efficiency at different values of torque and speed.

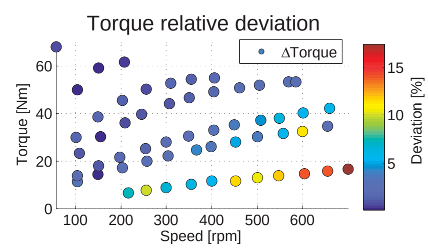


Fig. 6: Deviation in measured and calculated torque at different values of torque and speed.

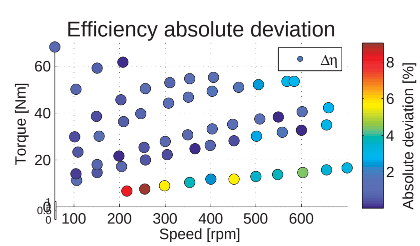


Fig. 7: Deviation in measured and calculated efficiency at different values of torque and speed.

Figure 6 shows the deviation in the calculation of the torque compared with measurements. The maximum deviation was estimated of approximately 17 %. In addition, the deviation in the calculation of the efficiency is illustrated in figure 7, with a maximum value of approximately 9 %. Various factors might be the source of such differences. In the case of the torque, the quality of the lamination might influence the performance of the machine regarding torque production. The deviations in the efficiency calculations are due to the absence of the mechanical losses in the simulation results. In addition, simulations do not account for processes such as cutting, stacking, etc. that might diminish the quality of the laminations, thus increasing the losses. Additionally, errors in the measurements may influence the deviations between measured and simulated efficiencies. Further analysis in this regard is presented in section V.

After contrasting the simulated values with the measurements, the magnet flux linked with the stator windings $\Psi_m$ was determined and the torque was obtained analytically with the expression:

$$T = \frac{3}{2}(\Psi_m \cdot I_q \cdot p) \tag{1}$$

Where $I_q$ is the current applied in the *q-axis* and $p$ is the pole-pairs number. This expression allows having torque values at currents that were not measured, enhancing the resolution for the elaboration of the efficiency maps. The copper losses $p_{cu}$ were obtained with the DC resistance of the windings $R_w$ and the measured current $I_m$ as:

$$p_{cu} = 3 \cdot I_m^2 \cdot R_w \tag{2}$$

For obtaining the stator and rotor iron losses and PM losses at any speed, quadratic fitting was applied to the losses calculated with 2D FEM simulations. Consequently, the efficiency was determined at any working point of the machine. The resulting efficiency map is presented in figure 8. This efficiency map agrees with the efficiency map of a Surface Mounted PM machine, which values of efficiency are higher as the machine is at its highest performance. In addition, it shows the incremental behaviour of the iron losses with the speed, and the increment of the copper losses with the increment of the torque.

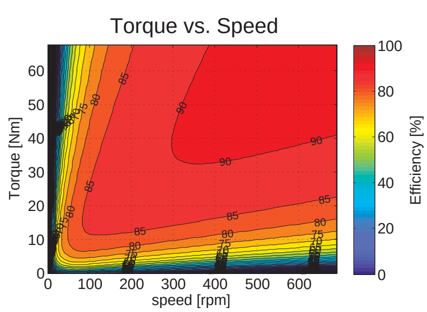


Fig. 8: Efficiency map of the original machine.

## IV. Study Case

The main goal of DEMETER project [12] is the study of the recyclability and reuse of magnets in (H)EVs. Therefore, a study case was defined in order to verify the methodology followed so far. Magnets manufactured with recycled material are expected to have lower remanence [13]. Hence, the remanence adopted for this study case was assumed to be 20 % lower, that is, $B_r = 0.96$ T. In order to perform a fair comparison, some assumptions were adopted for the study case presented here:

- Same geometry as in figure 4 was analysed. That is, similar values of current were applied to a new set of simulations with PMs of lower remanence.
- For performing a valid comparison, same performance in terms of torque production was required. Consequently, the axial length of the machine was increased by 15 %, that is, the new stack length was $L_{stack} = 46$ mm.
- The thermal aspects of having higher copper losses were disregarded for the analysis.

The procedure described previously was followed for the elaboration of the efficiency maps for this study case. Figure 9, illustrates the efficiency maps resulting from the use of assumed recycled magnets. Here it is observed the reduction of the efficiency in the region at low speed and high torque, where the copper losses are dominant. In the region at high speed low torque, where the no-load losses are dominant, the variation is less noticeable.

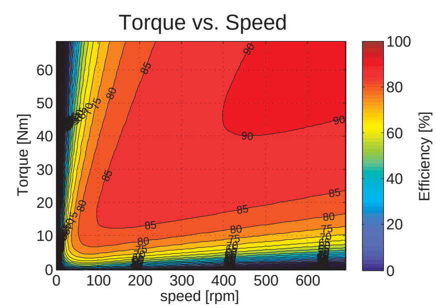


Fig. 9: Efficiency map of the machine for the study case.

### A. Comparison of efficiency maps

Figure 10 shows the deviations between the efficiency map for the original machine and the efficiency map obtained for the study case. The differences are more noticeable in the regions at high torque and low speed. That is, where the copper losses are dominant due to the higher current. In contrast, in regions at low torque and high speed, the deviations are lower. In this region the iron losses are dominant due to the higher frequency. However, the reduction of the iron losses due to the reduction of the remanence of the PMs is compensated by the increment of the length of the machine.

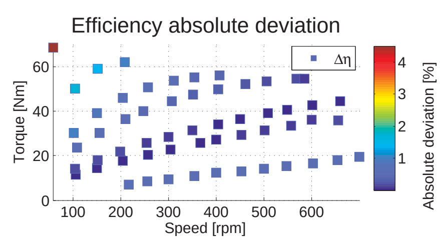


Fig. 10: Absolute error of efficiencies between efficiency map of original machine and machine with magnets of lower remanence.

## V. Results Analysis

This section is intended to enhance the understanding of the results in the presence of deviations between measurements and calculations. Furthermore, the analyses reported in this section were carried out on the original machine for similar values of torque and speed as for measurements. Hence, a decay test was performed on the original machine. It consisted in running the machine solely by pulling the shaft and recording the back-emf waveforms in an oscilloscope. A time decaying back-emf wave-form was obtained, and the no-load losses $p_{decay}$ (i.e. core losses, PM losses and mechanical losses) were obtained with the expression [14]:

$$p_{decay}(\omega_m) = -\omega_m J \frac{d\omega_m}{dt} \tag{3}$$

Where $J$ is the inertia of the machine and $\omega_m$ is the mechanical angular speed. The inertia $J$ was estimated with the main dimensions of the machine. The no-load losses as function of the speed of the machine were approximated by quadratic curve fitting. Figure 11 shows the decay test results, the calculated losses performed with 2D FEM and the measured no-load losses.

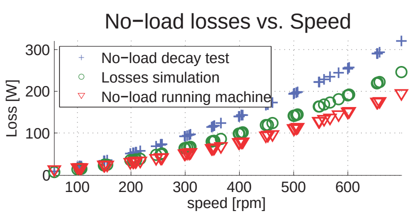


Fig. 11: Measured and calculated no-load losses in the original machine.

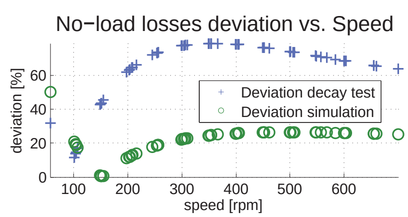


Fig. 12: Deviations in the no-load losses.

The deviations between measured and simulated results are shown in figure 12. The maximum deviation was estimated in approximately 50 %. The main source for this deviation would correspond to the portion of the mechanical and stray losses that are not included in the 2D FEM model. Additionally, the specific losses of the laminations in the actual machine remain unknown. Furthermore, as mentioned in section III the processing of the laminations (i.e. cutting, stacking, etc.) is not accounted in the simulations. Regarding the decay test results, figure 12 shows the largest deviations of approximately 79 %. The no-load losses $p_0$ with the machine running were determined with the following expression:

$$p_0 = P_m - P_o - p_{cu} \tag{4}$$

Where $P_m$ is the input power measured with the power analyser and $P_o$ is the output power obtained with the measurements of torque and speed in the torque transducer. Note that $p_0$ contains the mechanical losses, core losses and PM losses.

### A. *Effect of the calculation of J*

In order to evaluate the sensitivity of the value of inertia $J$ in the losses calculated with the decay test, $J$ was modified by $\pm 10$ %. The results are shown in figure 13.

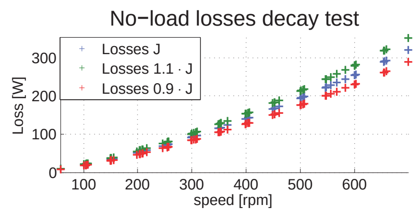


Fig. 13: Comparison of no-load losses with various values of inertia $J$.

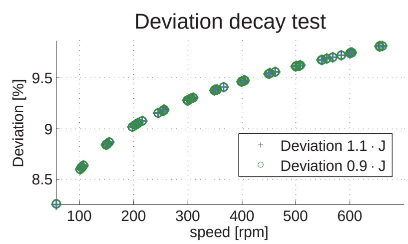


Fig. 14: Deviation of losses calculation with changing $J$.

As shown in figure 14 the maximum deviation was estimated in 10 %. In this work, the calculation of $J$ was performed both analytically and with the help of CAD software. The relative error between the two methods was approximately 3 %. The inertia calculated analytically was $J_{ana} = 0.0899$ kg·m$^2$. With CAD software, this value was estimated in $J_{cad} = 0.0905$ kg·m$^2$. The maximum calculated deviation due to the variation of the value of $J$ was estimated in 3 %.

### B. *Effect of the measurement of torque*

During the test with load in the machine, oscillations in the reading of torque were observed. In addition, an offset value was present in the interface used to read the values of torque. Such offset was identified having a value of approximately 0.35 Nm. The goal in this section is to identify the behaviour of the measured losses accounting for such deviations of the torque measurements. Hence, expression 4 was evaluated for the calculation of the no-load losses, accounting for the torque offset, by subtracting its value from the measurements. The results after applying quadratic curve fitting to the data are shown in figure 15 together with the decay test results and the values obtained with simulations.

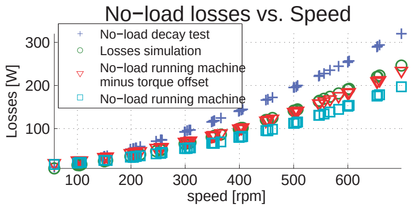


Fig. 15: No-load losses in the machine with torque offset.

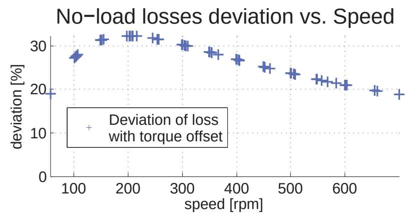


Fig. 16: Deviation in the no-load losses accounting for torque offset.

As it can be observed in figure 16, the subtraction of the torque offset from the measured values leads to the increment of the no-load losses. The maximum deviation between the decay test results and the measured values is of approximately 32 %. Which shows that the calibration of the torque transducer might have a significant impact in the estimation of the no-load losses as in equation 4. In addition, the losses calculated in 2D FEM are still close or even higher than the measured values. This might be the indication that in the original machine, an electrical lamination of lower specific losses was used. As future work, it would be interesting to determine the type of lamination that is being used by the manufacturer of this product.

## VI. Conclusions

A reduction of efficiency when recycled magnets are used was quantified at 4.5%. This maximum value was obtained in the region at low speed and high torque in figure 10. Such deviation in the efficiency has its source in the increment of the stack length for obtaining the same torque as in the original machine. In addition, the increment of the resistance of the windings with increased stack length, had a significant impact in the copper losses. On the other hand, in the region at high speed and low torque the reduction in efficiency was estimated in 1%. This is consistent with having a reduced remanence of the magnets compensated with the increment of the stack length of the machine.

In general, a larger consumption of energy is expected if magnets manufactured with recycled materials and with lower remanence are used for electrical machines in (H)EVs. However, for future work it has been defined the study of the energy consumption of the machine analysed here under various driving cycles, including the European urban driving cycle ECE-15. Additionally, the prices of both energy and magnet materials will be evaluated for establishing a recycling index [15]. Furthermore, the methodology proposed here is expected to facilitate the comparison of diverse types of PM machines (e.g. surface mounted PM, inset PM, Halbach rotor, etc.) from an early design stage.

## Acknowledgement

The research leading to the results presented in this article has been funded by the European Communitys Horizon 2020 Programme ([H2010/2014-2019]) under Grant Agreement no. 674973 (MSCA-ETN DEMETER). This publication reflects only the authors view, exempting the Community from any liability. Project website http://etn-demeter.eu/. Special thanks to professors Sylvie Hebert and Antoine Maignan for helping in the characterization of the magnets at the Laboratory of Cristallography and Material Sciences CRISMAT at ENSI-CAEN.

## References

[1] M. Kimiabeigi, R. S. Sheridan, J. D. Widmer, A. Walton, M. Farr, B. Scholes, and I. R. Harris, "Production and application of hpms recycled bonded permanent magnets for a traction motor application," *IEEE Transactions on Industrial Electronics*, vol. 65, no. 5, pp. 3795–3804, May 2018.

[2] S. Högberg, J. Holbøll, N. Mijatovic, B. B. Jensen, and F. B. Bendixen, "Direct reuse of rare earth permanent magnets - coating integrity," *IEEE Transactions on Magnetics*, vol. 53, no. 4, pp. 1–9, April 2017.

[3] S. Högberg, F. B. Bendixen, N. Mijatovic, B. B. Jensen, and J. Holbøll, "Influence of demagnetization-temperature on magnetic performance of recycled nd-fe-b magnets," in *2015 IEEE International Electric Machines Drives Conference (IEMDC)*, May 2015, pp. 1242–1246.

[4] Y. Yang, A. Walton, R. Sheridan, K. Güth, R. Gauß, O. Gutfleisch, M. Buchert, B.-M. Steenari, T. Van Gerven, P. T. Jones, and K. Binnemans, "Ree recovery from end-of-life ndfeb permanent magnet scrap: A critical review," *Journal of Sustainable Metallurgy*, vol. 3, no. 1, pp. 122–149, Mar 2017. [Online]. Available: https://doi.org/10.1007/s40831-016-0090-4

[5] T. Elwert, D. Goldmann, F. Roemer, and S. Schwarz, "Recycling of ndfeb magnets from electric drive motors of (hybrid) electric vehicles," *Journal of Sustainable Metallurgy*, vol. 3, no. 1, pp. 108–121, Mar 2017. [Online]. Available: https://doi.org/10.1007/s40831-016-0085-1

[6] A. Kumar Jha, Z. Li, A. Garcia Gonzalez, P. Upadhayay, and P. Rasmussen, "Weighted index of recycling and energy (WIRE) cost for Motors in electric vehicles," in *SPEEDAM 2018, Accepted*, 2017.

[7] T. Barlow, "A reference book of driving cycles for use in the measurement of road vehicle emissions: Version 3," 2009. [Online]. Available: https://books.google.dk/books?id=jnowMwEACAAJ

[8] S. M. Lukic and A. Emado, "Modeling of electric machines for automotive applications using efficiency maps," in *Proceedings: Electrical Insulation Conference and Electrical Manufacturing and Coil Winding Technology Conference (Cat. No.03CH37480)*, Sept 2003, pp. 543–550.

[9] P. Lazari, J. Wang, and L. Chen, "A computationally efficient design technique for electric-vehicle traction machines," *IEEE Transactions on Industry Applications*, vol. 50, no. 5, pp. 3203–3213, Sept 2014.

[10] K. Kiyota, H. Sugimoto, and A. Chiba, "Comparing electric motors: An analysis using four standard driving schedules," *IEEE Industry Applications Magazine*, vol. 20, no. 4, pp. 12–20, July 2014.

[11] "Wuxi lingming electric drive technology co., ltd," Internet: http://www.lingmingmotor.com, 2015, [Nov. 22, 2017].

[12] "European training network for the design and recycling of rare-earth permanent magnets," Internet: http://etn-demeter.eu, 2015, [Nov. 22, 2017].

[13] R. Sheridan, A. Williams, I. Harris, and A. Walton, "Improved hddr processing route for production of anisotropic powder from sintered ndfeb type magnets," *Journal of Magnetism and Magnetic Materials*, vol. 350, pp. 114 – 118, 2014. [Online]. Available: http://www.sciencedirect.com/science/article/pii/S0304885313007014

[14] A. Fitzgerald, C. Kingsley, and S. Umans, "Parameter determination from no-load and block-rotor tests," in *Electric Machinery*, 6th ed. New York, US: McGraw-Hill, 2003, ch. 6.

[15] P. Upadhayay, A. Garcia Gonzalez, Z. Li, A. Kumar Jha, P. Rasmussen, A. Kedous-Lebouc, and J.-C. Mipo, "Evaluation of energy cost index for an electric vehicle motor over a particular drive cycle with recycled magnet concept," in *ICEM 2018, Submitted to*, 2018.

## VII. Biographies

**Adolfo Garcia Gonzalez** received his M.Sc. degree in Electrical Engineering from KTH Royal Institute of Technology, Sweden, in 2015. He is currently working toward a Ph.D. degree at the Section of Electrical Machines of the Department of Energy Technology at Aalborg University. His research interests include modelling and design of electrical machines with 3D-Flux and non-traditional materials for traction applications.

**Amit Kumar Jha** received B.E degree (2008) in Electrical and Electronics Engineering from Birla Institute of Engineering, Mesra, India and M.Sc. degree (2012) in Electrical Power Engineering from Royal Institute of Technology, Stockholm, Sweden. He is currently working as Ph.D. researcher at G2Elab, Grenoble, France focusing on design of electrical motor with easy recycling for electric vehicles. Prior to PhD, he has worked in different companies like Bombardier Transportation AB, Vasteras, Sweden, Xylem water solutions, Stockholm, Sweden and Schneider Electric Pvt. Ltd, India. His fields of interest are design of electric motor and its drives for different motor applications and study system performance.

**Ziwei Li** received his M.Sc. degree in Electrical Engineering from KTH Royal Institute of Technology, Sweden, in 2015. He is currently working towards a Ph.D degree at the laboratory of G2Elab, Grenoble INP, Grenoble and Valeo - Equipements Electriques Moteur, Créteil, France. His research interests include modeling and optimization of radial flux electrical machines with rare earth magnets recycling concepts for electrical vehicle applications.

**Pranshu Upadhayay** was born in Jorhat, Assam, India in 1986. Following a B. Tech degree (2007) in Electrical Engineering from Nirma University, India, he received M. S. (Research) in Electrical Engineering (2015) from the Indian Institute of Technology Delhi, India. He is currently working towards his Ph.D. degree from G2Elab, Grenoble INP, Université Grenoble Alpes, and is also associated with Valeo - Equipements Electriques Moteur, Créteil, France. From 2007 to 2015 he was associated with multinational companies like Schneider Electric India Pvt. Ltd., and Crompton Greaves Ltd., at Mumbai, India. He has published 8 papers in International conference proceedings. His fields of interest include electrical machines and drives, design and FE analysis of special electrical machines, 3D flux claw-pole machines and rare earth magnet reuse and recycling concept in EV and HEV applications.

**Peter Omand Rasmussen** was born in Aarhus, Denmark, in 1971. He received the M.Sc.E.E. and Ph.D. degrees from Aalborg University, Aalborg, Denmark, in 1995 and 2001, respectively. In 1998, he became an Assistant Professor, and in 2002, he became an Associate Professor at Aalborg University. His research areas are the design and control of switched reluctance, permanent-magnet machines, and magnetic gears.